Magnetic phase transitions in Fe_2O_3–Bi_2O_3–B_2O_3 glasses

2008 J. Phys.: Condens. Matter 20 235216

(http://iopscience.iop.org/0953-8984/20/23/235216)

J. Phys.: Condens. Matter **20** (2008) 235216 (9pp) doi:10.1088/0953-8984/20/23/235216

Magnetic phase transitions in Fe_2O_3–Bi_2O_3–B_2O_3 glasses

Hirofumi Akamatsu, Katsuhisa Tanaka[1], Koji Fujita and Shunsuke Murai

Department of Material Chemistry, Graduate School of Engineering, Kyoto University, Nishikyo-ku, Kyoto 615-8510, Japan

E-mail: tanaka@dipole7.kuic.kyoto-u.ac.jp

Received 18 January 2008, in final form 9 April 2008
Published 6 May 2008
Online at stacks.iop.org/JPhysCM/20/235216

Abstract

Magnetic and structural properties of iron-containing bismuth borate glasses, whose composition is denoted as $x\mathrm{Fe_2O_3}\cdot(80.0-x)\mathrm{Bi_2O_3}\cdot 20.0\mathrm{B_2O_3}$, in mol% ($18.2 \leqslant x \leqslant 40.0$), have been explored. The glasses manifest intriguing magnetic behaviors explainable in terms of the coexistence of a spin glass phase and magnetic clusters. The $x = 18.2$ glass shows a spin glass transition at 3.5 K, while the contribution of magnetic clusters to the magnetic properties becomes more significant as the content of Fe_2O_3, x, is increased. We have performed detailed experiments on the $x = 32.0$ glass for which two different magnetic transitions are observed, as demonstrated by the temperature and frequency of the ac magnetic field dependences of the dc and ac susceptibilities. It is revealed from the measurements of magnetic ageing and memory effects that the magnetic clusters are frozen to form a superspin glass-like state with strong inter-cluster interactions at low temperatures. Transmission electron microscopy clarifies that the magnetic clusters are ascribable not to nanocrystals but to some phases possessing amorphous structures. Also, we have found from the observation of exchange bias effects that an interplay of the clusters with the spin glass phase brings about an exchange anisotropy field after cooling in the presence of magnetic field.

1. Introduction

Spin glass has been a subject of great interest since its experimental discovery in binary alloy systems such as *Au*Fe and *Cu*Mn, and many vigorous investigations have been carried out to clarify its intriguing magnetic properties [1, 2]. Even in this decade, fascinating phenomena involving magnetic ageing effects have been reported as unique characteristics of the spin glasses [3–14]. The spin glass system is also a matter of absorbing interest from a point of view of its analogy to many complex systems such as associative memory in the brain [15]. In binary alloy systems such as *Cu*Mn and *Au*Fe, categorized as canonical spin glasses, the magnetic moments of Mn and Fe atoms randomly distributed in the non-magnetic hosts are coupled with each other either ferromagnetically or antiferromagnetically via long-range RKKY (Ruderman–Kittel–Kasuya–Yosida) interaction mediated by conduction electrons, so magnetic frustrations are caused in the spin arrangement [16]. Both randomness and frustration are considered to be indispensable for the spin glass transition.

On the other hand, magnetic oxide glasses can be regarded as a system in which the magnetic moments localized at cations are randomly distributed in the insulating host glass structure. In addition to the random distribution of magnetic cations, magnetic frustrations can also occur in the configuration of magnetic moments because the short-range antiferromagnetic superexchange interaction is usually dominant in the oxide glasses and, in such a random structure, the antiferromagnetic interaction between two nearest-neighboring ions can be altered into ferromagnetic coupling by an additional magnetic ion present near to the two ions. Therefore, the magnetic oxide glass systems can satisfy the prerequisites for a spin glass transition. Actually, the freezing of randomly oriented magnetic moments was observed at very low temperatures in magnetic oxide glasses containing a sufficiently large amount of 3d transition metal ions such as Fe, Mn, and Co ions [3, 4, 17–22].

[1] Author to whom any correspondence should be addressed.

A mechanism of magnetic phase transition in oxide glasses has been discussed on the basis of experimental data. Verhelst *et al* [17] examined the temperature dependence of the ac susceptibility for $CoO–Al_2O_3–SiO_2$ glasses, and found that the ac susceptibility exhibited a cusp-like maximum at a certain temperature. They attempted to analyze the spin-freezing process by using a simple superparamagnetic model. Sanchez *et al* explained the temperature dependence of the relaxation time of the magnetic moments in $FeO–Al_2O_3–SiO_2$ [18] and $Li_2O–B_2O_3–Fe_2O_3$ [19] glasses in terms of the empirical Vogel–Fulcher relation instead of the Arrhenius law, suggesting that the simple superparamagnetic blocking cannot be imposed on the magnetic transition. Recently, we have demonstrated that binary $Fe_2O_3–TeO_2$ glasses manifest unique properties relevant to the spin dynamics including magnetic ageing and memory effects as well as critical slowing down [3]. These properties are similar to those observed in the canonical spin glasses such as *Au*–Fe alloys.

As mentioned above, the magnetic oxide glasses often exhibit transitions like those of spin glasses. On the other hand, ferromagnetic behaviors even at room temperature have been reported for some amorphous oxides containing Fe_2O_3 and Bi_2O_3 such as $Fe_2O_3–Bi_2O_3–ZnO$ [23], $Fe_2O_3–Bi_2O_3–CaO$ [24], $Fe_2O_3–Bi_2O_3–Li_2O$ [25, 26], and $Fe_2O_3–Bi_2O_3–CuO$ [27] systems, in the early 1990s. Nakamura *et al* [28] concluded that the ferromagnetic behavior in the $Fe_2O_3–Bi_2O_3–CaO$ and $Fe_2O_3–Bi_2O_3–Li_2O$ systems was attributable to some ferrimagnetic nanocrystalline phases embedded in the amorphous matrix, although the lattice images of the regions that they regarded as the nanocrystals in their transmission electron micrographs are not so clear. It should be noted that these iron-containing amorphous oxides do not exhibit any hyperfine sextet splittings in their Mössbauer spectra at room temperature, evidently suggesting that the ferromagnetic order does not extend over a long range, but is restricted to being within a localized region. Recently, we have reported on the magnetic structure of glass system containing Fe_2O_3 and Bi_2O_3 [4]. On the basis of the magnetic ageing and memory effects for the glass with the composition of $32.0Fe_2O_3{\cdot}48.0Bi_2O_3{\cdot}20.0B_2O_3$ (mol%), we disclosed a fascinating magnetic structure; there coexist a spin glass phase and magnetic clusters exhibiting superspin glass-like freezing at low temperatures. However, there still remain uncertainties as to the structural origin for the magnetic properties. Furthermore, it is of importance to examine the structure and magnetic properties of glasses with compositions different to $32.0Fe_2O_3{\cdot}48.0Bi_2O_3{\cdot}20.0B_2O_3$ so that the correlation among the composition, structure, and magnetic properties of the present oxide glass system can be clarified.

In the present paper, we describe experimental results, in detail, concerning magnetic and structural properties for $xFe_2O_3{\cdot}(80.0-x)Bi_2O_3{\cdot}20.0B_2O_3$ (mol%) glasses with $18.2 \leqslant x \leqslant 40.0$. We show that the magnetic behavior of $xFe_2O_3{\cdot}(80.0-x)Bi_2O_3{\cdot}20.0B_2O_3$ glasses is describable in terms of the spin glass transition due to individual magnetic moments of Fe^{3+} ions and/or small spin clusters as well as the glassy behavior of magnetic clusters where the spins of Fe^{3+} ions are locally frozen in very small regions; the glass with $x = 18.2$ consists of a spin glass phase at low temperatures, while the contribution of magnetic clusters to the magnetic properties becomes more significant with increase in the content of Fe_2O_3, x. The coexistence of a spin glass phase and magnetic clusters exhibiting superspin glass-like behavior is clearly reflected by the double transitions observed in the temperature dependence of the ac susceptibility. Detailed experiments on the $32.0Fe_2O_3{\cdot}48.0Bi_2O_3{\cdot}20.0B_2O_3$ glass reveal that the magnetic clusters are mainly amorphous and that very few clusters are attributable to nanocrystals. Although it may be naturally speculated that the glass will exhibit a spin glass transition when the concentration of magnetic ion is low and that the formation of magnetic clusters will prevail as the concentration of magnetic ions is increased, the variation of the magnetism with the concentration of magnetic ions has not been experimentally evidenced for any amorphous oxides as far as we know. This is partly because detailed properties relevant to the spin dynamics have never been clarified for any oxide glasses except for in our recent reports [3, 4]. In particular, the magnetic structure of the present glass system is unprecedented for the magnetic oxide glass systems in the sense that both a spin glass phase and magnetic clusters exhibiting a collective superspin glass-like freezing coexist in a single glass matrix.

2. Experimental details

Glasses whose nominal compositions are represented by $xFe_2O_3{\cdot}(80.0-x)Bi_2O_3{\cdot}20.0B_2O_3$, in mol% ($18.2 \leqslant x \leqslant 40.0$), hereafter denoted as xFeBiB for the convenience, were prepared from reagent grade Fe_2O_3, Bi_2O_3, and B_2O_3 powders by using a conventional melt-quenching method. Appropriate amounts of the starting materials were mixed thoroughly and the mixture was melted at 1150 °C for 1 h in a platinum crucible. The melt was poured onto a stainless steel plate and cooled in air. In order to explore the structural properties of the resultant glasses, x-ray diffraction (XRD) patterns were recorded by using Cu Kα radiation, and plan-view transmission electron microscope (TEM) observations were performed. ^{57}Fe Mössbauer spectroscopy was carried out at room temperature, employing ^{57}Co in metallic Rh as a γ-ray source, so as to estimate the valence states and coordination environments of Fe ions in the glasses. The velocity scale was calibrated by using the spectrum of α-Fe measured at room temperature. Magnetic properties including magnetic ageing and memory effects and the exchange bias effect were examined by using a superconducting quantum interference device (SQUID) magnetometer.

3. Results and discussion

3.1. X-ray diffraction and TEM observation

Figure 1 illustrates XRD patterns for 18.2FeBiB, 30.0FeBiB, 32.0FeBiB and 40.0FeBiB. The XRD diagram for 18.2FeBiB manifests only a halo pattern, suggesting that this sample is amorphous from the point of view of XRD. Only halo patterns seem to appear in the XRD diagrams of 30.0FeBiB

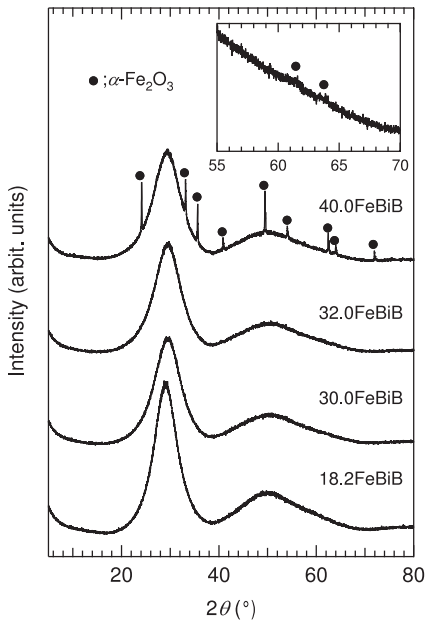

Figure 1. X-ray diffraction patterns of 18.2FeBiB, 30.0FeBiB, 32.0FeBiB and 40.0FeBiB. The inset illustrates a magnified XRD pattern for 32.0FeBiB in the range of $2\theta = 55°$–$70°$.

and 32.0FeBiB at a glance, although a careful look at these patterns reveals that very weak diffraction lines attributable to α-Fe_2O_3 are present at about $2\theta = 61.5°$ and 63.6° (see the inset of figure 1). The low intensity of these peaks indicates that the amount of α-Fe_2O_3 crystalline phase precipitated in these glasses is very small. Actually, TEM observation for 32.0FeBiB indicates that almost all the regions observed consist of an amorphous phase as shown in figures 2(a)–(c). We could find only one crystalline phase of about 10 nm in the plan-view observation for which we explored an area of about 10 μm^2 over the sample (figure 2(d)). The XRD pattern for 40.0FeBiB clearly depicts diffraction lines corresponding to α-Fe_2O_3 in addition to the halo pattern. The glass forming region of the present system obtained in this study is found to be smaller than those reported previously [29]. The amount of α-Fe_2O_3 precipitated is apt to increase with increasing value of x, as expected.

3.2. ^{57}*Fe Mössbauer spectroscopy*

The ^{57}Fe Mössbauer spectra for xFeBiB are shown in figure 3. The spectra for xFeBiB with $x < 40.0$ manifest a paramagnetic doublet attributable to Fe^{3+} ions, while absorption peaks due to Fe^{2+} ions are not observed. The spectrum for 40.0FeBiB clearly shows a hyperfine sextet as well as a paramagnetic doublet attributable to Fe^{3+} ions. The peak positions of the hyperfine sextet are identified as those of α-Fe_2O_3, consistently with the results from XRD. The values of the isomer shift for the paramagnetic Fe^{3+} ions are about 0.32 mm s^{-1} regardless of the value of x, suggesting that the Fe^{3+} ions mainly lie on the tetrahedral sites, surrounded by O^{2-} ions in the present glasses in contrast to the case for α-Fe_2O_3 where Fe^{3+} ions occupy the octahedral sites.

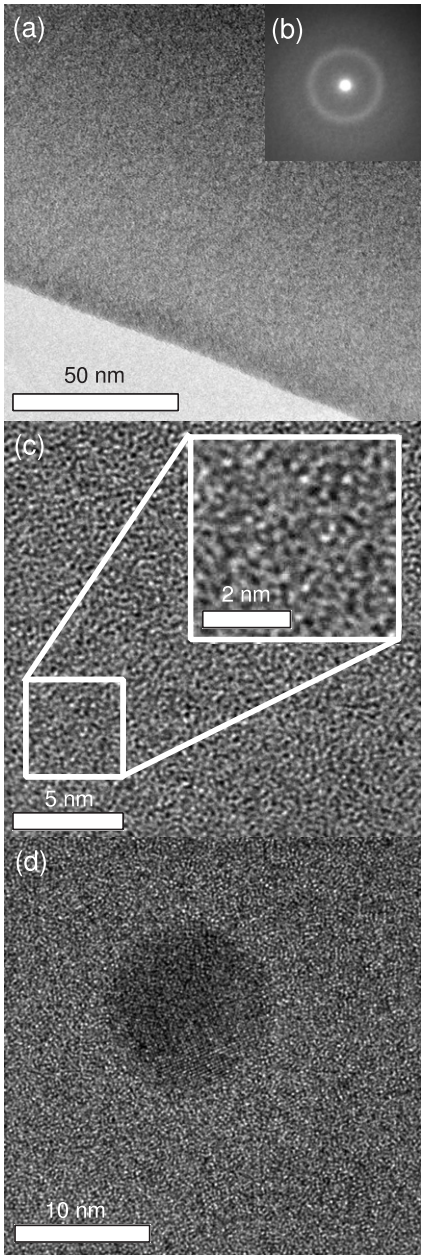

Figure 2. (a) TEM image and (b) selected area electron diffraction pattern of a typical region of 32.0FeBiB, and TEM image of (c) an amorphous region of 32.0FeBiB and (d) a nanocrystalline phase precipitated in the amorphous matrix.

3.3. *Temperature dependence of the dc susceptibility*

In figure 4, the dependence of the dc susceptibility on the temperature is illustrated for xFeBiB with varied x value. Both field cooling (FC) and zero-field cooling (ZFC) were performed with a magnetic field H_{dc} of 50 Oe applied. The temperature dependence of the dc susceptibility for 18.2FeBiB is similar to those observed for spin glasses; the susceptibility for ZFC shows a cusp-like maximum at $T_{cZFC} = 3.5$ K and the susceptibility for FC deviates from that for ZFC below T_{cZFC} (see figure 4(a)). This kind of behavior is also seen in other magnetic oxide glasses such as the Fe_2O_3–TeO_2 system [3, 21]. The inset of figure 4(a) depicts the inverse dc susceptibility as a

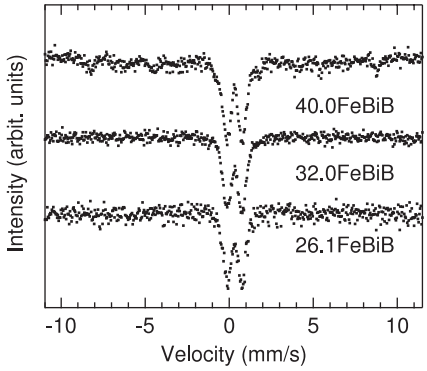

Figure 3. Mössbauer spectra of 26.1FeBiB, 32.0FeBiB and 40.0FeBiB at room temperature.

function of temperature for 18.2FeBiB. The linear relationship at high temperatures reveals that the glass is paramagnetic in the high temperature region; the linear part is describable in terms of the following Curie–Weiss law:

$$\frac{1}{\chi} = \frac{3k_{\mathrm{B}}\,(T-\theta)}{NM_{\mathrm{B}}^2\mu_{\mathrm{B}}^2}, \tag{1}$$

where χ is the dc susceptibility, T is the temperature, θ is the Weiss temperature, N is the number of magnetic ions per unit mass, μ_{B} is the Bohr magneton, M_{B} is the effective number of Bohr magnetons, and k_{B} is the Boltzmann constant. The dashed line represents the best fit of equation (1) to the experimental data with $M_{\mathrm{B}} = 4.7$ and $\theta = -97$ K. The value of M_{B} is significantly smaller than that expected from the spin-only value of the Fe^{3+} ion, i.e., 5.9. This implies that some of the magnetic moments of the Fe^{3+} ions form spin clusters at high temperatures near the room temperature. The negative value of θ means that the antiferromagnetic interaction is dominant among the Fe^{3+} ions in the glass. The ratio of θ to the Néel temperature or the spin glass transition temperature is regarded as a measure of magnetic frustration, i.e., a large ratio means a strong frustration, as discussed for a number of geometrically frustrated magnets [30]. In the present case, $|\theta|/T_{\mathrm{cZFC}} = 28$ is much larger than unity. A similar result was obtained for the $20.0Fe_2O_3{\cdot}80.0TeO_2$ (mol%) glass, for which $|\theta|/T_{\mathrm{cZFC}} = 16$ [21]. In oxide glasses, the antiferromagnetic superexchange interactions via oxide ions are predominant among the magnetic ions. A combination of these interactions with the random distribution of magnetic ions leads to the magnetic frustration which suppresses the magnetic transition toward lower temperatures.

In contrast to the sharp cusp observed for 18.2FeBiB, rather broad peaks at $T_{\mathrm{pZFC}} = 28$, 36 and 50 K are exhibited by the ZFC susceptibilities for xFeBiB with $x = 32.0$, 33.3 and 40.0, respectively (see figure 4(c)). It is noticeable that the ZFC and FC susceptibilities depart from each other just below 300 K, the highest measurement temperature in the present experiments. Such behaviors imply the presence of magnetic clusters similar to those observed in many magnetic nanoparticle systems with a wide distribution of particle size. A monotonic increase in T_{pZFC} with increasing x indicates that the higher the value of x, the larger the average volume of

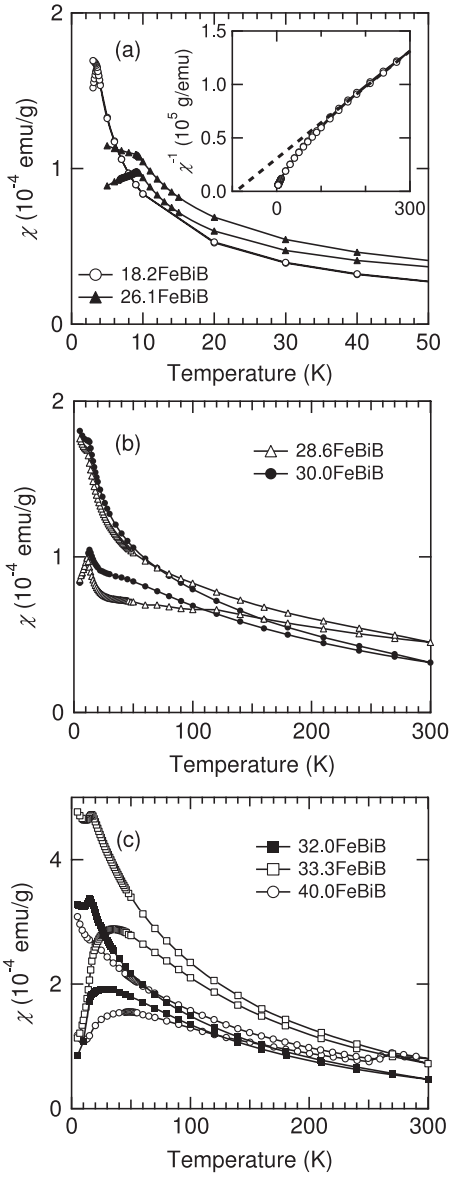

Figure 4. Temperature dependence of ZFC and FC dc susceptibilities for xFeBiB with (a) $x = 18.2$, 26.1, (b) 28.6, 30.0, (c) 32.0, 33.3 and 40.0 measured at $H_{\mathrm{dc}} = 50$ Oe. The inset of (a) shows the temperature dependence of the inverse dc susceptibility for 18.2FeBiB.

the magnetic clusters in xFeBiB. The ZFC susceptibility at T_{pZFC} for 40.0FeBiB is lower than those for 32.0FeBiB and 33.3FeBiB. This fact is attributable to the precipitation of α-Fe_2O_3, as clearly detected from the XRD measurement and the Mössbauer spectroscopy for 40.0FeBiB. This is also confirmed from figure 4(c), where the ZFC and FC susceptibilities for 40.0FeBiB show a dip in the temperature range from 270 to 250 K, suggesting that the magnetic behavior of 40.0FeBiB is significantly influenced by the α-Fe_2O_3 crystal, which has a magnetic anomaly called the Morin point at 250 K [31]. Therefore, the amount of Fe^{3+} ions present in the antiferromagnetic α-Fe_2O_3 phase is larger in 40.0FeBiB than in 32.0FeBiB and 33.3FeBiB, leading to the smaller ZFC susceptibility at T_{pZFC}. A close look at the FC susceptibility

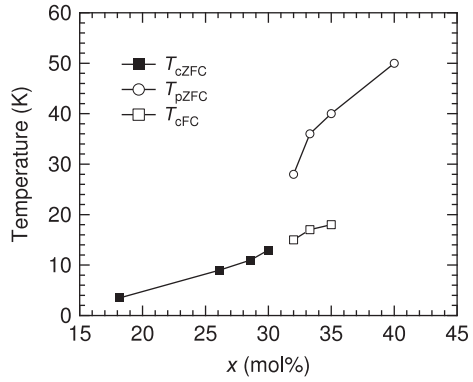

Figure 5. Variation of T_{cZFC}, T_{pZFC} and T_{cFC} with Fe_2O_3 content, x.

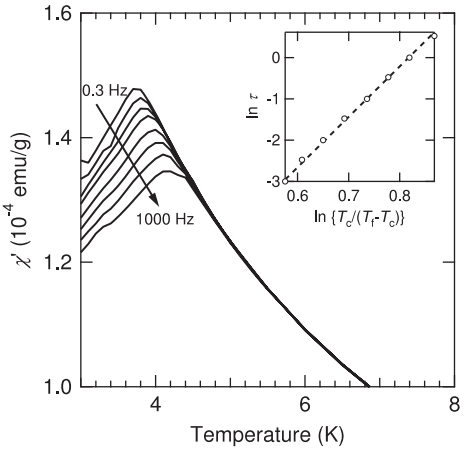

Figure 6. Temperature dependence of the real part of the ac susceptibility for 18.2FeBiB at $H_{ac} = 3$ Oe. The frequency f is 0.3, 1, 3, 10, 30, 100, 300 and 1000 Hz (from top to bottom). The inset illustrates the relationship between maximum relaxation time τ and spin-freezing temperature $T_f(f)$ based on the critical slowing down analysis.

curves for 32.0FeBiB and 33.3FeBiB reveals that cusp-like maxima are observed at $T_{cFC} = 15$ and 17 K, respectively. For both samples, T_{cFC} is lower than T_{pZFC}. As discussed later, T_{cFC} is thought to be a spin glass transition temperature.

As shown in figures 4(a) and (b), the susceptibility curves for 26.1FeBiB, 28.6FeBiB and 30.0FeBiB seem to be explained in terms of the coexistence of spin glass phases and magnetic clusters, the former and the latter of which are observed in 18.2FeBiB and 32.0FeBiB, respectively (see figures 4(a) and (c)). The ZFC susceptibilities for 26.1FeBiB, 28.6FeBiB and 30.0FeBiB manifest cusp-like maxima at $T_{cZFC} = 9$, 11 and 13 K, respectively, and the susceptibilities in the FC run separate from those in the ZFC run at temperatures much higher than T_{cZFC}.

Figure 5 illustrates the relationship between T_{cZFC}, T_{pZFC} and T_{cFC} and the content of Fe_2O_3, x. All the characteristic temperatures monotonically increase as x is increased. It is noteworthy that T_{cZFC} and T_{cFC} appear to lie on the same curve, although these two characteristic temperatures were evaluated through different procedures. This suggests that T_{cZFC} and T_{cFC} arise from the same origin, that is, a spin glass transition.

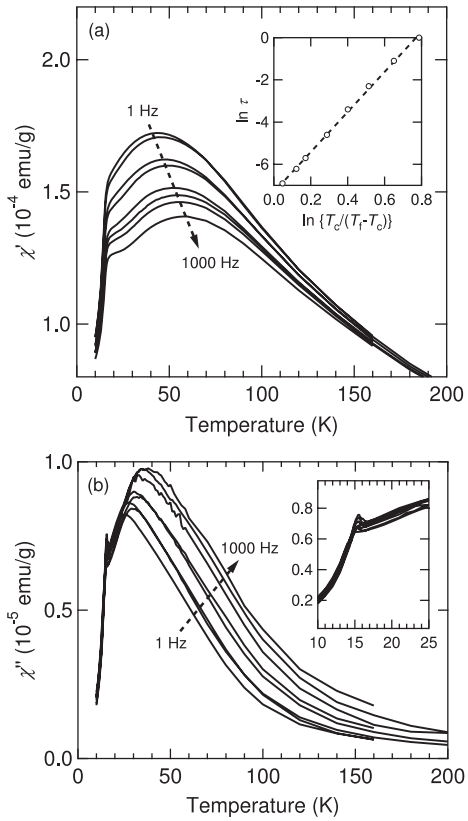

Figure 7. Temperature dependence of (a) real and (b) imaginary parts of the ac susceptibility for 32.0FeBiB at $H_{ac} = 3$ Oe. The frequency f is 1, 3, 10, 30, 100, 300, 500 and 1000 Hz (from top to bottom in (a) and vice versa in (b)). The inset of (a) illustrates the relationship between maximum relaxation time τ and spin-freezing temperature $T_f(f)$ based on the critical slowing down analysis. The inset of (b) shows a magnified view of the temperature variation of the imaginary part of the ac susceptibility in the range from 10 to 25 K.

3.4. Temperature dependence of the ac susceptibility

In order to elucidate the spin dynamics for the present glasses, the ac susceptibilities as a function of temperature were examined for 18.2FeBiB and 32.0FeBiB. The amplitude of the ac magnetic field H_{ac} was kept at 3 Oe and the ac frequency f was varied in the range from 0.3 to 1000 Hz. Figure 6 shows the temperature dependence of the real part of the ac susceptibility for 18.2FeBiB. As can be seen, the frequency-dependent spin-freezing temperature $T_f(f)$, defined as a temperature at which the real part of ac susceptibility manifests a maximum, shifts to the higher temperature side with increasing f. $T_f(f)$ corresponds to T_{cZFC} in the dc susceptibility for 18.2FeBiB. Figures 7(a) and (b) depict the temperature dependence of the real and imaginary parts of the ac susceptibilities for 32.0FeBiB, respectively. A systematic shift of the broad peak is obvious in figure 7(a). This peak stems from the same origin as T_{pZFC} in figure 4(c). In addition, a close inspection reveals that a shoulder and another peak appear in the real and imaginary parts of the ac susceptibilities for 32.0FeBiB, respectively, in the temperature range below $T_f(f)$ (see the inset of figure 7(b)). This corresponds to the cusp-like maximum at $T_{cFC} = 15$ K in the FC curve of the dc susceptibility (see figure 4(c)).

The relative shift of $T_f(f)$ per decade of f, i.e., $\Psi = (\Delta T_f/T_f)/\Delta(\log f)$ [16], for the real part of the ac susceptibility was determined as 0.029 and 0.085 for 18.2FeBiB and 32.0 FeBiB, respectively. The former value is in the range of those obtained for the spin glasses, i.e., $\sim 10^{-3}$–10^{-2}, while the latter value is in an intermediate range between the spin glass and the superparamagnet values, i.e., $\sim 10^{-1}$ [16, 32, 33]. For the magnetic transition in the vicinity of $T_{cFC} = 15$ K in 32.0FeBiB, it is difficult to evaluate the value of Ψ in the same way as mentioned above, because the real part of the ac susceptibility does not exhibit a distinguishable peak, but appears as a shoulder near T_{cFC}. However, $\Psi = 0.017$ could be roughly determined by setting T_f equal to the peak temperature of the out-of-phase component. The value suggests that the transition near T_{cFC} can be categorized as a spin glass transition.

The analysis of the data in terms of the power law,

$$\tau = \tau_0 \left(\frac{T_f(f) - T_c}{T_c} \right)^{-z\nu}, \tag{2}$$

based on the dynamic scaling hypothesis yields $z\nu = 11.9$, $T_c = 3.3$ K and $\tau_0 = 1.6 \times 10^{-10}$ s for 18.2FeBiB and $z\nu = 9.5$, $T_c = 30$ K and $\tau_0 = 6.6 \times 10^{-4}$ s for 32.0FeBiB. The value of $z\nu$ for 18.2FeBiB is comparable with the typical values for canonical spin glasses [34, 35], while τ_0 is slightly longer than the spin flip time of individual magnetic moments belonging to atoms or ions, i.e., 10^{-13}–10^{-12} s, implying that small spin clusters are involved in the spin glass transition of 18.2FeBiB. On the other hand, the value of $\tau_0 = 6.6 \times 10^{-4}$ s for 32.0FeBiB is similar to but somewhat larger than those reported for strongly interacting nanoparticle systems and superspin glasses, for which $\tau_0 \sim 10^{-6}$ s [34, 36]. The larger value of $\tau_0 (= 10^{-4.7}$ s) was reported for Fe_xC_{1-x} ($x \sim 0.2$–0.3) nanoparticles dispersed in xylene with the volume fraction of 5 vol%, suggesting that the behavior was attributable to a mixture of collective and single-particle dynamics [36]. It was proposed that the strong inter-particle interactions arising from the regions where the number density of the particles is higher than its average may enhance the local correlation length and render the relaxation time longer than expected from the volume fraction of particles when a homogeneous dispersion is assumed. For 32.0FeBiB, both cooperative and non-cooperative characteristics are also seen: the former appear in the magnetic ageing and memory effects as observed in the strongly interacting nanoparticle systems and superspin glasses (shown below), and the latter are reflected by the absence of a plateau of the FC susceptibility below T_{pZFC} as observed for the non-interacting superparamagnets. Therefore, in the present case, the local correlation of magnetic clusters can contribute to the larger value of τ_0.

The Vogel–Fulcher empirical law,

$$\tau = \tau_0 \exp\left(\frac{E_a}{k_B (T - T_0)} \right), \tag{3}$$

where E_a is the activation energy and T_0 represents an inter-cluster interaction or a true transition temperature, has been used to analyze the temperature dependence of the relaxation time for the spin glasses and interacting nanoparticle systems. Fitting the Vogel–Fulcher equation to the experimental data yields reasonable parameter values of $\tau_0 = 1.0 \times 10^{-7}$ s, $E_a/k_B = 320$ K and $T_0 = 25$ K. On the other hand, the analysis by using the Arrhenius law:

$$\tau = \tau_0 \exp\left(\frac{E_a}{k_B T} \right), \tag{4}$$

results in the fitting parameters of $\tau_0 = 1.3 \times 10^{-12}$ s and $E_a/k_B = 1200$ K. The activation energy seems to be too large. The fact that the Vogel–Fulcher law can explain the experimental data better than the Arrhenius law also evidences the existence of inter-cluster interactions in 32.0FeBiB.

3.5. ZFC memory effects

To get an insight into the nature of the magnetically ordered phase of 32.0FeBiB, we have performed the zero-field cooling memory experiment proposed by Mathieu *et al* [5]. In this experiment, the system is cooled in zero magnetic field from high temperature with or without a long stop at a specific temperature T_s situated below the transition temperature. $\chi(T)$ is recorded during the subsequent heating in a measuring magnetic field. Sasaki *et al* [37] have demonstrated that a memory is imprinted during the ageing in the absence of magnetic field only for spin glasses and strongly interacting nanoparticle systems or superspin glasses, and not for non-interacting superparamagnets. Hence, the observation of the memory effect is confirmation of a cooperative spin dynamics [33, 37–43].

The detailed protocol is the same as that previously reported [4] except for the stopping temperatures (T_s). The differences in $\chi(T)$ between the cases with and without the long stop are plotted in figure 8 for varied T_s. The memory effect is clearly seen as a dip at T_s. As T_s becomes lower than 15 K, the memory dip becomes much narrower and deeper. Although it is difficult to consider this phenomenon quantitatively, the memory dips observed under the condition that $T_s > 15$ K are reasonably ascribable to the superspin glass-like freezing of magnetic clusters, while those at $T_s < 15$ K are due to the spin glass phase which emerges below about 15 K [4]. The observation of the memory dip at $T_s > 15$ K clearly rules out the occurrence of a two-step phase transition of a single magnetic component. This is because if one magnetic phase showed a two-step transition, the spin configuration grown by the ageing at $T_s > 15$ K would be forced to change into a completely different configuration state as the temperature was decreased below 15 K, and as a result, the memory effect would disappear. We have performed a ZFC memory experiment to verify that two magnetic phases coexist in the present system. The system was cooled down to 12 K ($< T_{cFC} = 15$ K) at which it was aged for 3 h in zero magnetic field, and cooled down to 5 K after heating up to 17 K ($> T_{cFC} = 15$ K). Subsequently, the magnetic field of 50 Oe was applied and $\chi(T)$ was measured on heating. The result is shown in the inset of figure 8. The ageing effect imprinted at 12 K does not vanish completely after heating up to 17 K. This fact indicates that the dip observed at 12 K consists of two

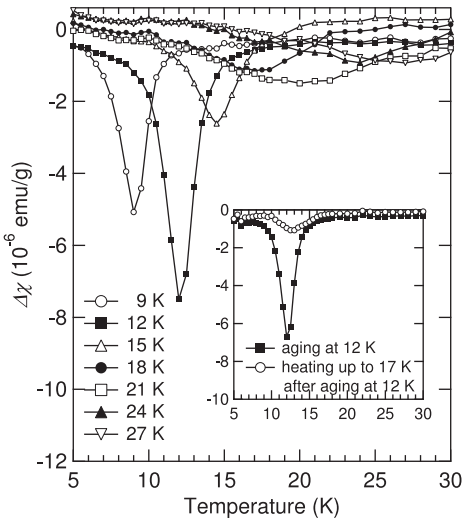

Figure 8. Temperature variation of the difference in susceptibility for 32.0FeBiB between the cases with and without ageing for 3 h at each of the stopping temperatures. The susceptibilities were measured on heating after zero-field cooling with or without the ageing. The inset shows the temperature dependence of the difference in susceptibility between the cases with and without ageing for 3 h at 12 K (closed squares). The open circles denote the ageing at 12 K and subsequent heating to 17 K.

components at least and supports the idea that the system does not undergo any two-step magnetic phase transitions.

One question remains: whether the magnetic clusters are to be identified as the crystalline phase of α-Fe_2O_3 detected via the XRD and TEM. Clusters composed of other crystalline phases such as γ-Fe_2O_3 and Fe_3O_4 are also possible. As far as magnetic nanoparticle systems are concerned, the memory effect imprinted during the ageing in zero field has been observed only for those cases with the number density of the nanoparticles being very large. For instance, in the $Co_{80}Fe_{20}/Al_2O_3$ multilayer system [38], no ZFC memory effects were observed for the thin film even when the volume fraction of the magnetic phase was as high as 14 vol%, where CoFe particles with the average diameter of about 1.8 nm were precipitated inside the Al_2O_3 matrix and the separation between the particles was about 10 nm. In the present case, the volume fraction of the crystalline phase detected from the XRD measurement and the TEM observation is so small that the magnetic clusters exhibiting the collective dynamics including the ZFC memory effect cannot be ascribed to the crystalline phase. We conjecture the origin of magnetic clusters in the present system as follows. Some Fe ion-rich regions are produced in the amorphous matrix during the process of melt-quenching, since the driving force for forming α-Fe_2O_3 brings about certain microscopic concentration fluctuations of Fe ions, and some parts of such regions are frozen as amorphous clusters before the crystallization into α-Fe_2O_3. The regions enriched with Fe^{3+} ions in the amorphous matrix are responsible for the superspin glass transition. The other regions in the amorphous matrix undergo the spin glass transition at low temperatures. We emphasize that the magnetic clusters present as the amorphous phase can lead to the superspin glass freezing assisted by the strong inter-cluster interactions even at room temperature, as depicted in figure 4. A similar phenomenon was reported for amorphous oxides with high Fe^{3+} ion concentrations such as amorphous Fe_2O_3, in which the superspin glass-like behavior was observed even at room temperature [44].

3.6. Exchange bias-like effect

An exchange bias effect is peculiar to an interface between two magnetic phases such as ferromagnet/antiferromagnet and ferromagnet/spin glass interfaces [45–50]. The exchange bias is a shift of the magnetic hysteresis loop when the system containing such magnetic interfaces is cooled down in an external magnetic field from a certain temperature below the Curie temperature to a temperature below the Néel temperature or the spin-freezing temperature. At the interface, the magnetic moments of antiferromagnets or spin glasses are coupled with those of ferromagnets oriented in the direction of the external magnetic field, leading to a unidirectional anisotropy along the magnetic field. Also, the exchange interactions at the interfaces usually enhance the coercivity of ferromagnets. Recently, the exchange bias has been measured to confirm the interface exchange coupling in magnetically phase-separated manganites and cobaltates [45, 46]. We have performed exchange bias measurements for 32.0FeBiB, which is composed of two magnetic components, i.e., the spin glass and the magnetic clusters exhibiting superspin glass transition. In this case, we should use the term 'exchange bias-like effects' instead of 'exchange bias effects' because we do not discuss the conventional ferromagnetic hysteresis loops but magnetic hysteresis cycles within the non-ergodic low temperature region peculiar to the spin glasses. In the present experiments, the magnetic field dependence of the magnetization was measured after cooling in the magnetic field of 0.5 T from 300 K to the measurement temperature. The magnetization measurements were performed in magnetic fields of -3 to 3 T. In this system, in contrast to the ferromagnet/spin glass systems often studied for the exchange bias effects, the magnetization is not saturated even in high magnetic fields. So we fixed the highest measurement magnetic field at 3 T, where the hysteresis loops are completely closed at any temperature, and the cooling field was set to 0.5 T, much lower than 3 T. Figure 9(a) shows the dependence of the magnetization on the magnetic field at 5 K. The central region of figure 9(a) is magnified in figure 9(b). It is found that the magnetic hysteresis loop shifts along the field axis. We define the coercive field H_c and the exchange bias-like field H_{ex} as $(H_2 - H_1)/2$ and $(H_2 + H_1)/2$, respectively, where H_1 and H_2 are the negative and positive magnetic fields at which the magnetization is equal to zero, as shown in figure 9(b). H_{ex} and H_c are plotted against temperature in figure 9(c). H_{ex} shows very small but non-zero values above $T_{cFC} = 15$ K at which the spin glass transition takes place, and increases drastically below 15 K. H_c exhibits a temperature dependence similar to that of H_{ex}. The magnitude of the exchange bias-like field becomes larger as the superspin glass-like freezing of the magnetic clusters gradually proceeds with decrease in the temperature.

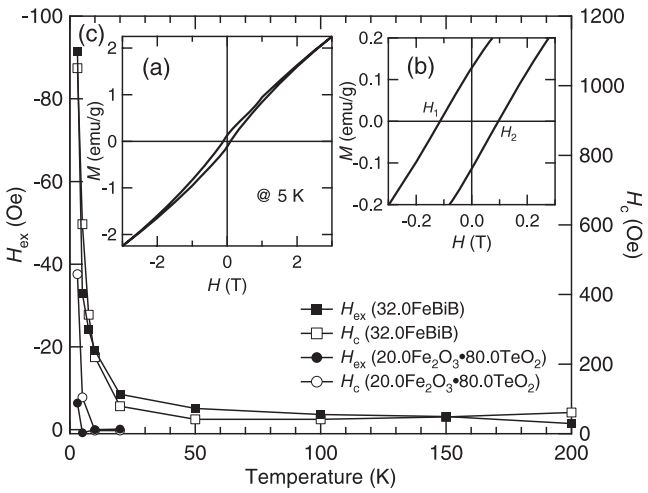

Figure 9. (a) Variation of magnetization with magnetic field measured for 32.0FeBiB at 5 K. (b) Enlarged view of the central region of (a). (c) Temperature dependence of the exchange bias field, H_{ex} (closed square and circle), and coercive field, H_c (opened squares and circles), for 32.0FeBiB and $20.0Fe_2O_3{\cdot}80.0TeO_2$ glass.

The enhancements of the exchange anisotropy and coercive force presumably indicate the emergence of interface exchange coupling between the magnetic clusters and the spin glass phase. The metastable alignment of superspins formed under the FC condition is thought to exert a positive internal magnetic field on the atomic spin glass phase. However, the finite values of H_{ex} may be explainable in terms of the fact that the exchange bias-like effect is one of the intrinsic properties of spin glasses and related materials such as cluster spin glasses and superspin glasses [47]. We must explore both possibilities. As a reference for the intrinsic exchange bias-like effect in a simple amorphous oxide spin glass, we have examined the exchange bias-like effect in the same procedure for the glass with the nominal composition of $20.0Fe_2O_3{\cdot}80.0TeO_2$ (mol%), which exhibits a spin glass transition at $T_g = 9$ K [3, 21]. For the $20.0Fe_2O_3{\cdot}80.0TeO_2$ glass, H_{ex} is actually equal to zero above 5 K ($=0.6T_g$) and $H_{ex} = -6$ Oe and $H_c = 459$ Oe are obtained at 3 K ($=0.3T_g$), as shown in figure 9(c). In the case of 32.0FeBiB, an abrupt rise of H_{ex} is observed just below T_{cFC}, and the amplitude of H_{ex} at 5 K ($=0.3T_{cFC}$) for 32.0FeBiB is five times larger than that at 3 K ($=0.3T_g$) for the $20.0Fe_2O_3{\cdot}80.0TeO_2$ glass. Therefore, the temperature dependence of H_{ex} for 32.0FeBiB is not well explained simply in terms of the inherent nature of the spin glass phase emerging at T_{cFC}. The present glass can be regarded as one of the exchange bias-like systems possessing no clear structural interfaces, as confirmed by the TEM observation, but having interfaces among the magnetic phases.

4. Conclusion

For the $xFe_2O_3{\cdot}(80.0 - x)Bi_2O_3{\cdot}20.0B_2O_3$ (mol%) glass system with $18.2 \leqslant x \leqslant 40.0$, the magnetic structure depends on the content of Fe_2O_3. The magnetic behavior of 18.2FeBiB is similar to that of the canonical spin glasses. In the cases where the content of Fe_2O_3 is above 26.1 mol%, the glasses are composed of two magnetic components, i.e., the spin glass phase and magnetic clusters manifesting a superspin glass transition. As the value of x increases, the contribution of magnetic clusters to the magnetic properties becomes more remarkable. Our careful investigations, including the ZFC memory experiments and the TEM observation for 32.0FeBiB, suggest that the magnetic clusters strongly interact with each other, assisting the occurrence of a superspin glass transition, and that the clusters are mainly present as an amorphous state. It is revealed from the measurements of the exchange bias effect that the interplay of the spin glass phase with the magnetic clusters leads to the formation of an exchange anisotropy field after the field cooling. Compared with the magnetic oxide glass systems reported so far, the present glass system has novel magnetic structure in the sense that there exist two magnetic ordered phases interacting with each other.

Acknowledgments

The authors would like to thank Professor S Kitagawa of the Graduate School of Engineering, Kyoto University, for magnetization measurements and Dr M Tosaki of the Radioisotope Research Center, Kyoto University, for the Mössbauer effect measurements. This research was partially supported by the Ministry of Education, Science, Sports and Culture, Grant-in-Aid for Scientific Research (B), 19360298, 2007.

References

[1] Cannella V and Mydosh J A 1972 *Phys. Rev.* B **6** 4220
[2] Nagata S, Keesom P H and Harrison H R 1979 *Phys. Rev.* B **19** 1633
[3] Akamatsu H, Tanaka K, Fujita K and Murai S 2006 *Phys. Rev.* B **74** 012411
[4] Akamatsu H, Tanaka K, Fujita K and Murai S 2007 *J. Magn. Magn. Mater.* **310** 1506
[5] Mathieu R, Jönsson P, Nam D N H and Nordblad P 2001 *Phys. Rev.* B **63** 092401
[6] Jonason K, Vincent E, Hammann J, Bouchaud J P and Nordblad P 1998 *Phys. Rev. Lett.* **81** 3243
[7] Jonsson T, Jonsson K, Jönsson P and Nordblad P 1999 *Phys. Rev.* B **59** 8770
[8] Jönsson P, Hansen M H and Nordblad P 2000 *Phys. Rev.* B **61** 1261
[9] Jonason K, Nordblad P, Vincent E, Hammann J and Bouchaud J-P 2000 *Eur. Phys. J.* B **13** 99
[10] Bernardi L W, Yoshino H, Hukushima K, Takayama H, Tobo A and Ito A 2001 *Phys. Rev. Lett.* **86** 720
[11] Dupuis V, Vincent E, Bouchaud J-P, Hammann J, Ito A and Katori H A 2001 *Phys. Rev.* B **64** 174204
[12] Miyashita S and Vincent E 2001 *Eur. Phys. J.* B **22** 203
[13] Jönsson P E, Mathieu R, Nordblad P, Yoshino H, Katori H A and Ito A 2004 *Phys. Rev.* B **70** 174402
[14] Jönsson P E, Yoshino H, Nordblad P, Aruga Katori H and Ito A 2002 *Phys. Rev. Lett.* **88** 257204
[15] Hopfield J J 1982 *Proc. Natl Acad. Sci. USA* **79** 2554
[16] Mydosh J A 1993 *Spin Glasses: An Experimental Introduction* (London: Taylor and Francis)
[17] Verhelst R A, Kline R W, de Graaf A M and Hooper H O 1975 *Phys. Rev.* B **11** 4427
[18] Sanchez J P, Friedt J M, Horne R and Van Duyneveldt A J 1984 *J. Phys. C: Solid State Phys.* **17** 127

[19] Sanchez J P and Friedt J M 1982 *J. Physique* **43** 1707
[20] Shaw J L, Wright A C, Sinclair R N, Marasinghe G K, Holland D, Lees M R and Scales C R 2004 *J. Non-Cryst. Solids* **345/346** 245
[21] Tanaka K, Akamatsu H, Nakashima S and Fujita K 2008 *J. Non-Cryst. Solids* **354** 1346
[22] Hayashi M, Suga M and Nagata K 1999 *J. Appl. Phys.* **85** 2257
[23] Ota N, Okubo M and Masuda S 1986 *J. Magn. Magn. Mater.* **54–57** 293
[24] Nakamura S and Ichinose N 1987 *J. Non-Cryst. Solids* **95/96** 849
[25] Nakamura S and Ichinose N 1989 *Japan. J. Appl. Phys.* **28** 984
[26] Chen J, Cheney S and Srinivasan G 1994 *J. Appl. Phys.* **75** 6828
[27] Soeya S, Nakamura S and Ichinose N 1990 *J. Appl. Phys.* **68** 2875
[28] Nakamura S, Hirotsu Y and Ichinose N 1991 *Japan. J. Appl. Phys.* **30** L844
[29] Qiu H H, Ito T and Sakata H 1999 *Mater. Chem. Phys.* **58** 243
[30] Ramirez A P 1994 *Annu. Rev. Mater. Sci* **24** 453
[31] Morin F J 1950 *Phys. Rev.* **78** 819
[32] Antic B, Goya G F, Rechenberg H R, Kusigerski V, Jovic N and Mitric M 2004 *J. Phys.: Condens. Matter* **16** 651
[33] Sahoo S, Petracic O, Kleemann W, Stappert S, Dumpich G, Nordblad P, Cardoso S and Freitas P P 2003 *Appl. Phys. Lett.* **82** 4116
[34] Djurberg C, Svedlindh P, Nordblad P, Hansen M F, Bodker F and Morup S 1997 *Phys. Rev. Lett.* **79** 5154
[35] Gunnarsson K, Svedlindh P, Nordblad P, Lundgren L, Aruga H and Ito A 1988 *Phys. Rev. Lett.* **61** 754
[36] Hansen M F, Jönsson P E, Nordblad P and Svedlindh P 2002 *J. Phys.: Condens. Matter* **14** 4901
[37] Sasaki M, Jönsson P E, Takayama H and Mamiya H 2005 *Phys. Rev.* B **71** 104405
[38] Chen X, Bedanta S, Petracic O, Kleemann W, Sahoo S, Cardoso S and Freitas P P 2005 *Phys. Rev.* B **72** 214436
[39] Sahoo S, Petracic O, Kleemann W, Nordblad P, Cardoso S and Freitas P P 2003 *Phys. Rev.* B **67** 214422
[40] Cador O, Grasset F, Haneda H and Etourneau J 2004 *J. Magn. Magn. Mater.* **268** 232
[41] Sankar C R and Joy P A 2005 *Phys. Rev.* B **72** 132407
[42] Du J, Zhang B, Zheng R K and Zhang X X 2007 *Phys. Rev.* B **75** 014415
[43] Nair S, Nigam A K, Narlikar A V, Prabhakaran D and Boothroyd A 2006 *Phys. Rev.* B **74** 132407
[44] Shafi K, Ulman A, Yan X, Yang N, Estournès C, White H and Rafailovich M 2001 *Langmuir* **17** 5093
[45] Niebieskikwiat D and Salamon M B 2005 *Phys. Rev.* B **72** 174422
[46] Tang Y K, Sun Y and Cheng Z H 2006 *Phys. Rev.* B **73** 174419
[47] Nogués J and Schuller I K 1999 *J. Magn. Magn. Mater.* **192** 203
[48] Del Bianco L, Fiorani D, Testa A M, Bonetti E and Signorini L 2004 *Phys. Rev.* B **70** 052401
[49] Ali M, Adie P, Marrows C H, Greig D, Hickey B J and Stamps R L 2007 *Nat. Mater.* **6** 70
[50] Martínez B, Obradors X, Balcells L, Rouanet A and Monty C 1998 *Phys. Rev. Lett.* **80** 181